CFD Modelling of a Fluid Flowing Inside a Channel

Student number: 17004291

March 22, 2019

Abstract

This projects uses CFD simulations to investigate the pattern of fluid flow for two cases; fluid flowing inside a channel and fluid encountering a rectangular beam in a confined flow. The former is investigated both analytically and numerically, whereas the latter only has a numerical solution due to the non-linearity of the underlying PDE describing the flow. Following the application of boundary conditions, iterative finite difference algorithms are used in conjunction with successive overrelaxation methods (SOR) to obtain the solutions. The relaxation parameter is optimised for both solutions. Laminar flow patterns are obtained for both cases, and in the latter turbulent flow is also observed when the grid Reynolds number is increased. This behaviour is linked to the terms of the Navier-Stokes equation, namely the viscous and convective terms.

Contents

Theory

1.1 Introduction

Fluid dynamics is of key interest to many different branches of physical sciences, ranging from mathematics to aeronautics. Their mathematical interest stems from the fact that the central equations governing the behaviour of fluids are non-linear differential equations. Therefore, except for simple cases, where certain assumptions can be applied to simplify the expressions, there exists no analytic solutions. This motivates physical scientists to seek numerical solutions to model fluid flow, most often through a computational approach.

This project investigates the flow of a fluid for two different cases. Firstly, the channel flow is examined by simulating the behaviour of a 'river' when two thin plates are submerged into it. This particular case has an analytic solution following the application of boundary conditions. Therefore, both an analytic and a numerical solution is produced for the motion and compared. Secondly, the behaviour of a **viscous** fluid is investigated as it flows and encounters a beam (blockage) that distracts its flow.

The rest of the theory section covers the mathematical background for the project with all the relevant equations, whereas the method section explains the computational approach used in the investigation. We start with the most central equation; the **Navier-Stokes equation** and derive the rest of the equations from it.

1.2 Navier-Stokes Equation

The flow of a general, compressible fluid is famously given by the Navier-Stokes equation: [1]

$$\rho \frac{D\mathbf{v}}{Dt} = \rho \mathbf{F} - \nabla p + \mu \nabla^2 \mathbf{v} \tag{1.1}$$

$\frac{D\mathbf{v}}{Dt}$ is a special time derivative, also known as **the hydrodynamic derivative**.

$$\frac{D\mathbf{v}}{Dt} = (\mathbf{v} \cdot \nabla)\mathbf{v} + \frac{\partial \mathbf{v}}{\partial t} \tag{1.2}$$

If we define viscosity in the following way;

$$\mu = \rho \nu \tag{1.3}$$

, the Navier-Stokes equation can be rearranged to give:

$$(\mathbf{v} \cdot \nabla)\mathbf{v} + \frac{\partial \mathbf{v}}{\partial t} = \mathbf{F} + \nu\nabla^2\mathbf{v} - \frac{1}{\rho}\nabla p \tag{1.4}$$

$(\mathbf{v} \cdot \nabla)\mathbf{v}$ is the transport of momentum due to fluid flow, also called the convective term.
$\frac{\partial \mathbf{v}}{\partial t}$ is time gradient of the velocity of the fluid.
$\mathbf{F}$ is a source term.
$\nu\nabla^2\mathbf{v}$ is the viscous term.
$\frac{1}{\rho}\nabla p$ is the pressure gradient.

1.3 Velocity field equations

1.3.1 Continuity equation

Continuity equation is obtained from the Navier-Stokes equation by applying the special conditions. Firstly, the fluid is assumed to be **inviscid**, **incompressible** and in a **steady state** with a **constant pressure gradient**. Therefore, the **density**, ρ, of the fluid is **constant**, the **viscosity** is **zero** and the velocity of the fluid does not depend on time. There is no source term, therefore $\mathbf{F}$ is also zero. Thus, the effects of any outside forces, such as gravity, are assumed to be negligible. After cancelling the relevant terms, the following relation is obtained:

$$(\mathbf{v} \cdot \nabla)\mathbf{v} = 0 \tag{1.5}$$

As the velocity is non-zero, the continuity equation is found to be:

$$\nabla \cdot \mathbf{v} = 0 \tag{1.6}$$

In two-dimensions, it is given as:

$$\frac{\partial v_x}{\partial x} + \frac{\partial v_y}{\partial y} = 0 \tag{1.7}$$

1.3.2 Momentum equations

By applying the relevant assumptions on the Navier-Stokes equation, we obtain the momentum equations, one for each dimension. The fluid is assumed to be **incompressible** and in a **steady state**, however **viscous** this time. There is no source term.

After cancelling the relevant terms and rearranging, the following relation is obtained:

$$\nu\nabla^2\mathbf{v} = (\mathbf{v} \cdot \nabla)\mathbf{v} + \frac{1}{\rho}\nabla p \tag{1.8}$$

The two momentum equations for the x and y-components of a two-dimensional velocity field are given below:

$$\nu\left(\frac{\partial^2 v_x}{\partial x^2} + \frac{\partial^2 v_x}{\partial y^2}\right) = v_x\frac{\partial v_x}{\partial x} + v_y\frac{\partial v_x}{\partial y} + \frac{1}{\rho}\frac{\partial p}{\partial x} \tag{1.9}$$

$$\nu\left(\frac{\partial^2 v_y}{\partial x^2}+\frac{\partial^2 v_y}{\partial y^2}\right)=v_x\frac{\partial v_y}{\partial x}+v_y\frac{\partial v_y}{\partial y}+\frac{1}{\rho}\frac{\partial p}{\partial y} \tag{1.10}$$

1.4 Vorticity

Vorticity in fluids is analogous to angular momentum of solids. The vorticity vector, **w**, is the curl of the velocity vector **v**. The approach used in investigating vorticity is relating the velocity field, **v**, to a potential (also called the **stream function**), **u**, as given below:[2]

$$\mathbf{v}=\nabla\times\mathbf{u} \tag{1.11}$$

The potential only has a z-component, $\mathbf{u}=\mathbf{u}(0,0,u)$. Substituing this into (1.11) gives:

$$\mathbf{v}=\left(\frac{\partial u}{\partial y},\frac{-\partial u}{\partial x},0\right) \tag{1.12}$$

The vorticity is given by the following equation.

$$\mathbf{w}=\nabla\times\mathbf{v} \tag{1.13}$$

Therefore, **w** is given by:

$$\mathbf{w}=-\nabla^2\mathbf{u} \tag{1.14}$$

, or in two-dimensions:

$$\frac{\partial^2 u}{\partial x^2}+\frac{\partial^2 u}{\partial y^2}=-w \tag{1.15}$$

The fluid is still assumed to be **incompressible** and in a **steady state**, however the effects of vorticity will no longer be ignored. Equation (1.4), in this case, simplifies to:

$$\nu\nabla^2\mathbf{v}=(\mathbf{v}\cdot\nabla)\mathbf{v} \tag{1.16}$$

In 2D:

$$\nu\left(\frac{\partial^2 w}{\partial x^2}+\frac{\partial^2 w}{\partial y^2}\right)=\frac{\partial u}{\partial y}\frac{\partial w}{\partial x}-\frac{\partial u}{\partial x}\frac{\partial w}{\partial y} \tag{1.17}$$

(1.15) and (1.17) form the basis of the code implemented in investigating the vorticity around a beam along the path of a laminar flow.

Method

2.1 Part I - Channel flow

Figure 2.1: Channel flow between two submerged thin plates (with specified boundary conditions)[3]

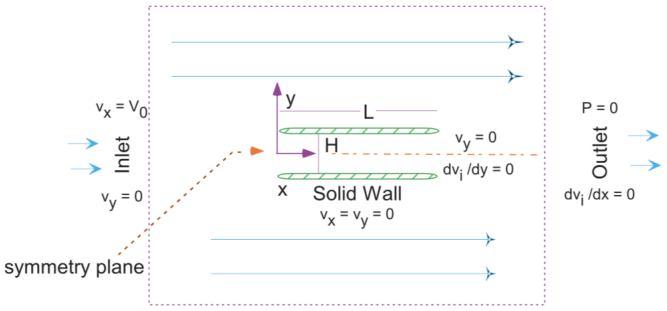

To investigate the flow represented in figure 2.1 , **equations (1.7), (1.9)** and **(1.10)** are used. Boundary conditions are applied to simplify these expressions in order to reach an analytic result. Furthermore, some of these conditions provide the basis of the iterative process used in the numerical approach to find a solution. Table 2.1 illustrates the boundary conditions used.

Table 2.1: Boundary conditions in channel flow

Boundary condition	**Effect**
Solid plates	No-slip boundary conditions: $v_x = v_y = 0$ at the plates surface.
Inlet	The fluid velocity at the inlet is unchanged: $v_x = V_0$
Outlet	Zero fluid pressure: $P = 0$ and $\frac{\partial v_x}{\partial x} = 0$, $\frac{\partial v_y}{\partial x} = 0$
Symmetry plane	Symmetrical about the centre $v_y = 0$ and $\frac{\partial v_y}{\partial y} = 0$

2.1.1 Analytic solution

The boundary conditions in table 2.1 are applied to simplify **equations (1.7), (1.9)** and **(1.10)**. The following expressions are obtained.

Continuity equation:

$$\frac{\partial v_x}{\partial x} = 0 \tag{2.1}$$

Momentum equations:

$$\rho\nu \frac{\partial^2 v_x}{\partial y^2} = \frac{\partial p}{\partial x} \tag{2.2}$$

$$\frac{\partial p}{\partial y} = 0 \tag{2.3}$$

(2.2) is integrated twice and no-slip boundary conditions are applied to find the two constants of integration. The velocity is found to be:

$$v_x = \frac{1}{2\nu\rho}\frac{\partial p}{\partial x}(y^2 - yH) \tag{2.4}$$

(2.4) is used to plot a laminar channel flow for reference and compare the analytic velocity values with the numerical ones. The plots can be found in the results section.

2.1.2 Numerical approach

v_y is assumed to be zero following the application of the boundary conditions, therefore a horizontal laminar flow is being investigated. Momentum equation for v_y, (1.10), cancels out. Therefore, only (1.9) is non-trivial. This is an elliptic PDE. The finite difference form of (1.9) is as follows:

$$\begin{aligned} 4v_x(i,j) = v_x(i+1,j) + v_x(i-1,j) + v_x(i,j+1) + v_x(i,j-1) \\ -\frac{h}{2}v_x(i,j)[v_x(i+1,j) - v_x(i-1,j)] \\ -\frac{h}{2}[p(i+1,j) - p(i-1,j)] \end{aligned} \tag{2.5}$$

An iterative process is needed to scan the mesh for all indices i and j and update the values of v_x, until a certain level of convergence. The method used here is the **successive overrelaxation method (SOR)**, which calculates a residual at each scan and adds it to the velocity field. A relaxation parameter, ω, is included to scale the residual in an attempt to speed up the convergence. An optimal value for ω exists and a range of values between $0 < \omega < 2$ are investigated. The full update regime is given below: [4]

$$v_x(i+1,j) = v_x(i-1,j) \tag{2.6}$$

$$r(i,j) = \frac{1}{4}\Big(v_x(i+1,j) + v_x(i-1,j) + v_x(i,j+1) + v_x(i,j-1)\Big) \tag{2.7}$$

$$-\frac{h}{8}v_x(i,j)[v_x(i,j+1) - v_x(i,j-1)] - \frac{h}{8}[p(i+1,j) - p(i-1,j)] - v_x(i,j)$$

$$v_x(i,j) = v_x(i,j) + \omega r(i,j) \tag{2.8}$$

(2.6) is the boundary condition at the outlet imposed iteratively.

The finite difference form of the pressure gradient has a simple form:

$$p(i+1,j) - p(i-1,j) = \frac{\partial p}{\partial x} \times 2\Delta h \tag{2.9}$$

2.2 Part II - A beam in a confined flow

The case where there is a blockage along the flow of a fluid is investigated. As mentioned later as part of the boundary conditions, this type of flow is assumed to be symmetric about the centreline of the beam. Therefore, only half the plane is considered in this investigation and the plots are presented accordingly. Relevant equations are (1.15) and (1.17).[3]

Figure 2.2: Half-plane of a beam in a confined flow

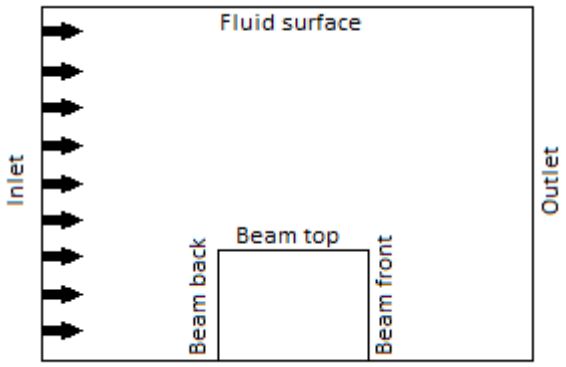

2.2.1 Numerical approach - Finite difference equations

The approach used here is the same as for part I. However, there are now two update schemes; one for the stream function, **u** and one for the vorticity field, **w**. The finite difference form of (1.15) is:

$$\frac{u(i+1,j)+u(i-1,j)+u(i,j+1)+u(i,j-1)-4u(i,j)}{h^2}=-\omega \tag{2.10}$$

The finite difference form of (1.17) is:

$$\nu\left(\frac{w(i+1,j)+w(i-1,j)+w(i,j+1)+w(i,j-1)-4w(i,j)}{h^2}\right) \tag{2.11}$$

$$=\frac{u(i+1,j)-u(i,j)}{h}\frac{w(i+1,j)-w(i,j)}{h}-\frac{u(i+1,j)-u(i,j)}{h}\frac{w(i+1,j)-w(i,j)}{h}$$

The full SOR update scheme with two residuals is:

$$u(i,j)=u(i,j)+\omega r^{(1)}(i,j) \tag{2.12}$$

$$w(i,j)=w(i,j)+\omega r^{(2)}(i,j) \tag{2.13}$$

$$r^{(1)}(i,j)=\frac{1}{4}(u(i+1,j)+u(i-1,j)+u(i,j+1)+u(i,j-1)+h^2w(i,j)) \tag{2.14}$$

$$-u(i,j)$$

$$r^{(2)}(i,j)=\frac{1}{4}\Big(w(i+1,j)+w(i-1,j)+w(i,j+1)+w(i,j-1) \tag{2.15}$$

$$-\frac{R}{4}\Big[[u(i,j+1)-u(i,j-1)][w(i+1,j)-w(i-1,j)]$$

$$-[u(i+1,j)-u(i-1,j)][w(i,j+1)-w(i,j+1)]\Big]\Big)-w(i,j)$$

Vorticity field, $w(i,j)$ should not be confused with the relaxation parameter, ω .

The stream function is plotted to illustrate the potential field of the flow. In order to better investigate the motion of the fluid arrows representing the velocity field should also be plotted so that any curls (vortices) can be visualised. Equation (1.12) gives the relationship between the velocity field and stream function. The finite difference form of the stream function is found and used to plot the velocity field arrows on top of the potential field.

2.2.2 Boundary conditions

In this system, there are a number of boundary conditions imposed by the borders of the flow and also the borders of the beam placed inside the fluid. The equations representing the flow in this case are elliptic PDEs with open surfaces, therefore, both **Dirichlet and Neumann conditions** are used to solve them numerically. The former utilises the value of the solution on a surrounding closed surface, whereas the latter uses the value of the normal derivative on the surrounding surface. Tables 2.2 and 2.3 illustrate the mathematical constraints imposed at all the boundaries. [3]

Table 2.2: Boundary conditions at the borders

Border	**Equations**
Fluid surface	$u(i+1,j)=u(i,j)+V_0h$ and $w(i,j)=0$
Inlet	$u(i+1,j)=u(i,j)$ and $w(i,j)=0$
Centreline	$u(i,j)=0$ and $w(i,j)=0$
Outlet	$u(i+1,j)=u(i,j)$ and $w(i+1,j)=w(i,j)$

Table 2.3: Boundary conditions at the surfaces of the beam

Beam surface	**Equations**
Back surface	$u(i,j)=0$ and $w(i,j)=\frac{-2\left(u(i+1,j)-u(i,j)\right)}{h^2}$
Top surface	$u(i,j)=0$ and $w(i,j)=\frac{-2\left(u(i,j+1)-u(i,j)\right)}{h^2}$
Front surface	$u(i,j)=0$ and $w(i,j)=\frac{-2\left(u(i-1,j)-u(i,j)\right)}{h^2}$

Results and discussion

3.1 Part I - Channel flow

Figure 3.1: Analytic solution of channel flow with velocity values shown in the colourbar.

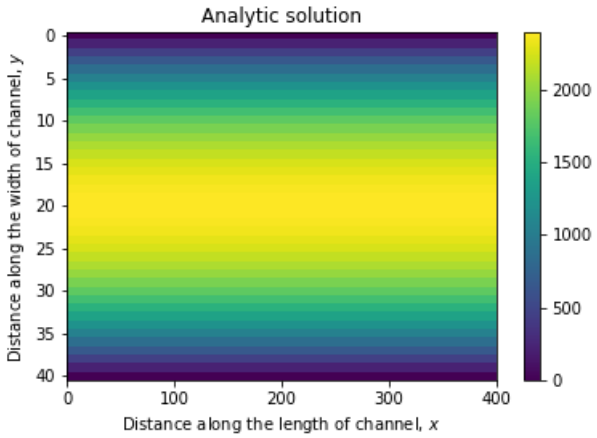

Figure (3.1) illustrates a typical analytic solution of the channel flow. The motion of an incompressible fluid down a parallel-sided channel is driven by a (negative) pressure gradient between the inlet and outlet. Constant pressure gradient was assumed in this system. The velocity field is expected to be independent of x along the channel, therefore it only depends on y. The colours in the plot clearly show that the velocity along x is a parabola in y, with maximum value at the centre and no velocity at all along the top and bottom borders (no-slip conditions).

By inspecting the image plots qualitatively in figure (3.2), it is clear to see that the velocity at the inlet is always constant as this is imposed. Through iterative updates, the steady state solution representing channel flow slowly forms as x increases. It should be noted that the length of the channel has been extended from 400 to 4000, so that the solution can form within the range. The image gets progressively more similar to the analytic plot.

Figure 3.2: Numerical solutions of channel flow for $0.2 \leq \omega \leq 1.8$. The image plots illustrate the form of flow with the magnitude of velocities indicated on the colorbars. The image plots illustrate the velocity values for analytic and numerical solutions explicitly.

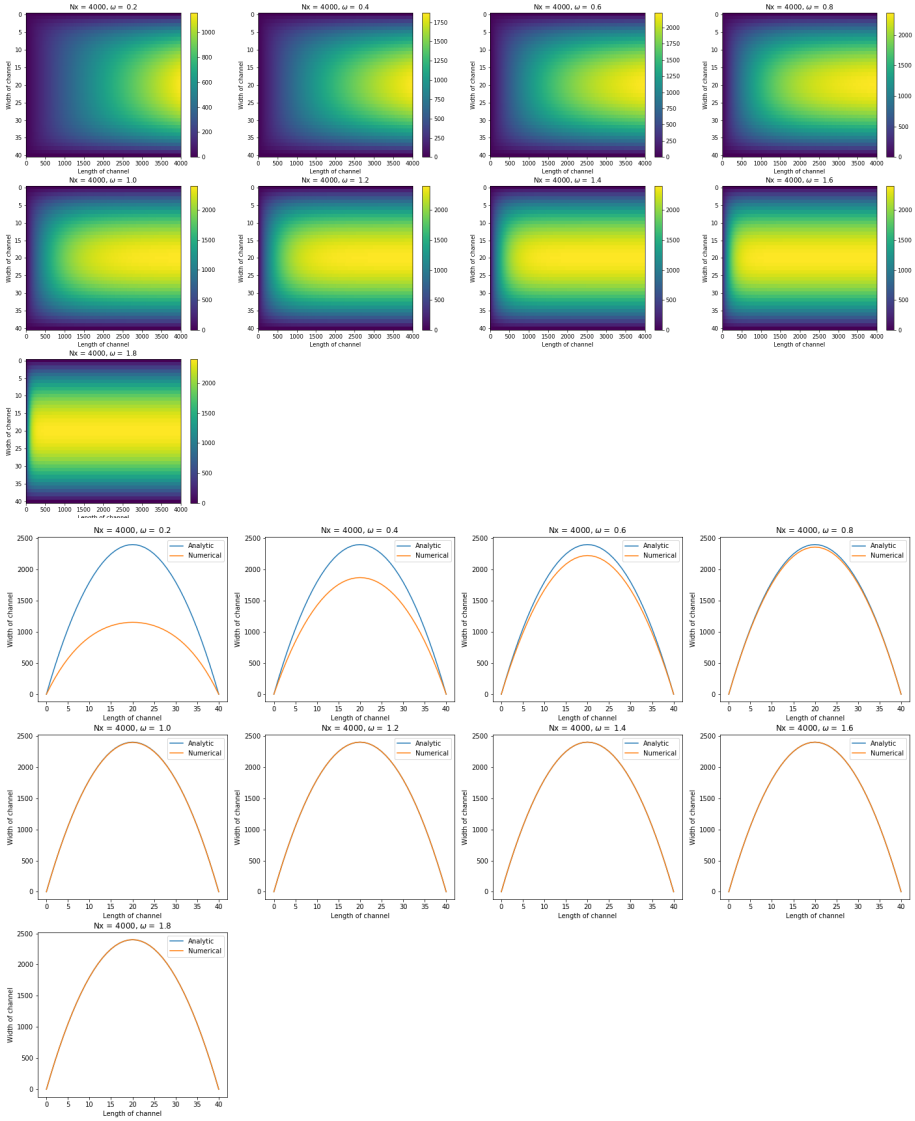

The line graphs in figure (3.2) enable a quantitative comparison of both solutions. The velocities along the end-point of the numerical solutions for different ω are taken and plotted within the same axes as the velocity values from the analytic solution. Full convergence has occurred for $\omega \geq 1.0$. The number of iterations necessary to form the solutions for $\omega = 0.2, 0.4, 0.6, 0.8, 1.0, 1.2, 1.4, 1.6, 1.8$ were $75, 38, 24, 17, 12, 12, 19, 33, 70$ respectively. Therefore, the optimal value for the relaxation parameter lies in the range $1.0 \leq \omega \leq 1.2$.

3.2 Part II - A beam in a confined flow

Figure 3.3: The flow illustrated in a small grid. Colours on the plot indicate the magnitude of the stream function at all points and the arrows illustrate the velocity field.

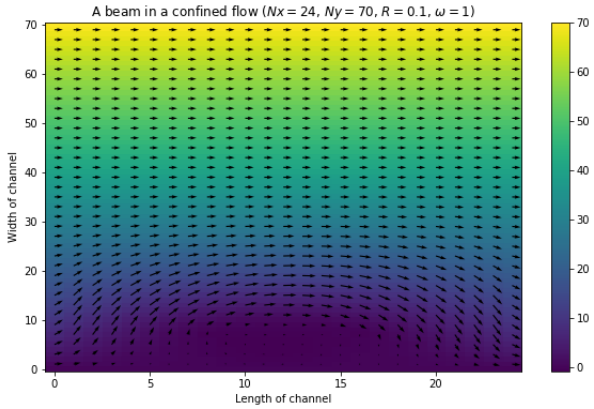

Fig.(3.3) is the initial plot using a small grid. The flow is smooth as can be seen form the shape formed by the arrows. After this initial plot, the effect of changing different specified parameters on the flow was investigated.

Firstly, the effect of changing the relaxation parameter on the efficiency of the process and on the convergence of the solution was investigated. For $\omega = 0.2, 0.4, 0.6, 0.8, 1.0, 1.2, 1.4, 1.6$, the number of iterations required were $286, 180, 137, 113, 96, 81, 65$. $\omega > 1.6$ has given numerical instabilities with the solution diverging. A finer investigation has shown that the most efficient value of ω is 1.5 which led to the solution to convergence after 54 iterations.

Secondly, the size of the mesh was increased in the x-direction to give the flow more space downstream of the beam. The beam is placed very close to the inlet relative to the new length of the channel. Fig.(3.4) shows the flow for $Nx = 300$ and $dbeam = 20$, where Nx is the length of the channel and $dbeam$ is the distance from the inlet to the beam.

Figure 3.4: Flow in a grid extended along the x-direction.

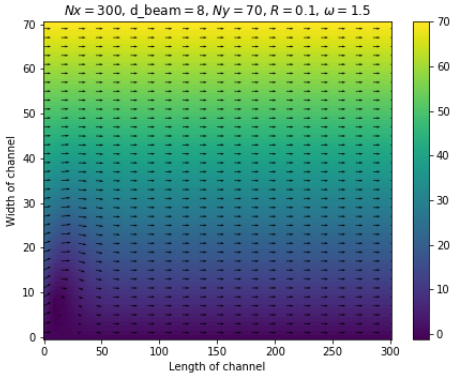

In order to fully observe the effects of increasing R, the length of the channel was increased from 24 to 100 and ω was taken as 0.3. For large values of ω, larger values of R result in numerical instabilities. For instance, if $\omega = 1$, the solution diverges for $R > 1$. Fig.(3.5) illustrates the flow for increasing R when the beam was placed at $dbeam = 20$. The beam was then moved to $dbeam = 50$ to give flow more space upstream of the beam and investigate the behaviour. Both the stream functions and the vorticity fields were plotted for this case.

Figure 3.5: The effect of increasing R on the flow. The beam is at dbeam= 20.

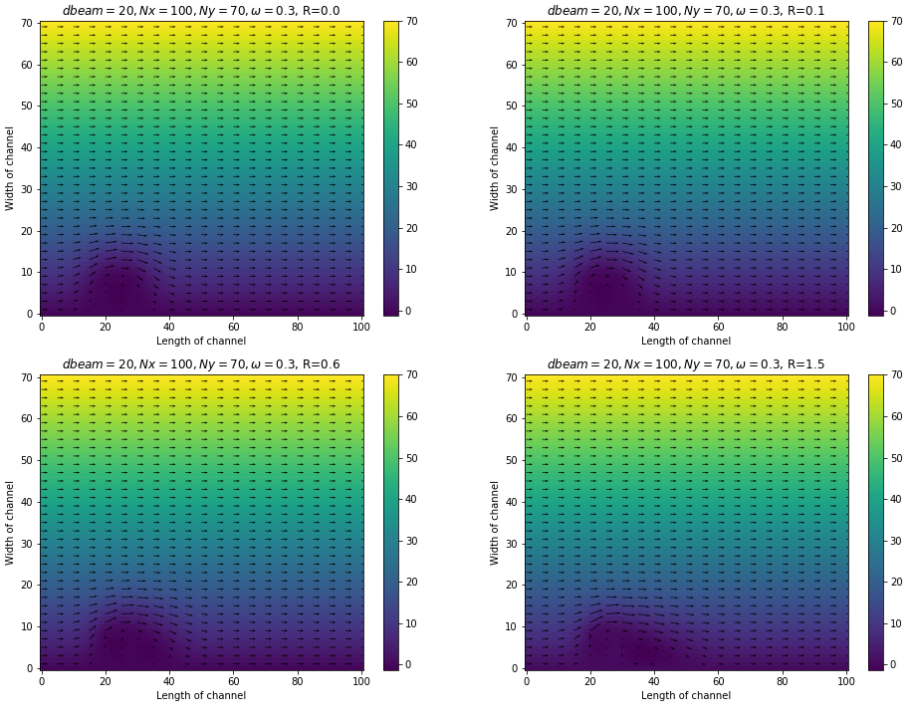

Figure 3.6: The effect of increasing R on the stream function and on the vorticity field. The beam is at dbeam = 50.

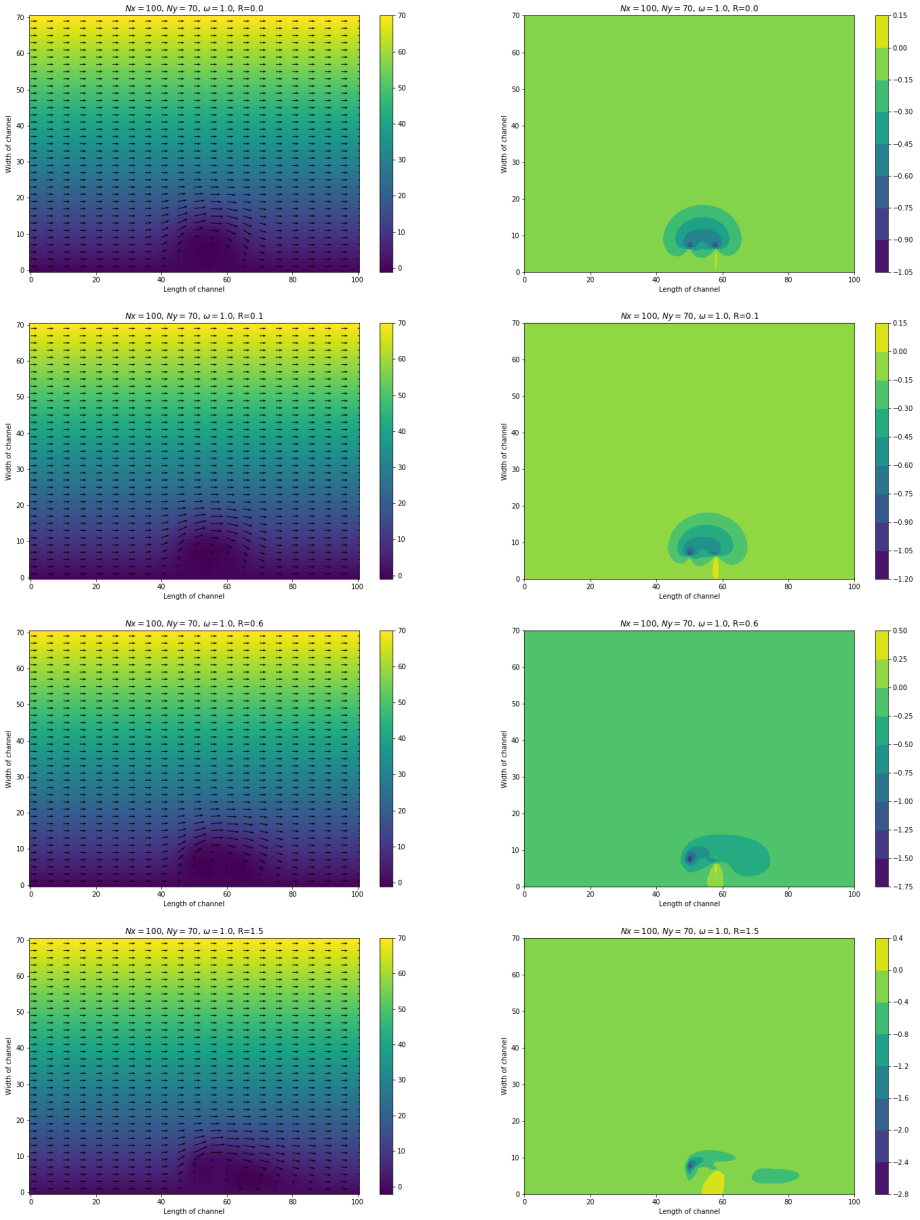

The last plots ($R = 1.5$) are showing an interesting behaviour. Fig.(3.6) is the same stream function plot with a larger scale.

Figure 3.7: Flow for R=1.5. A vortex forms downstream of the beam.

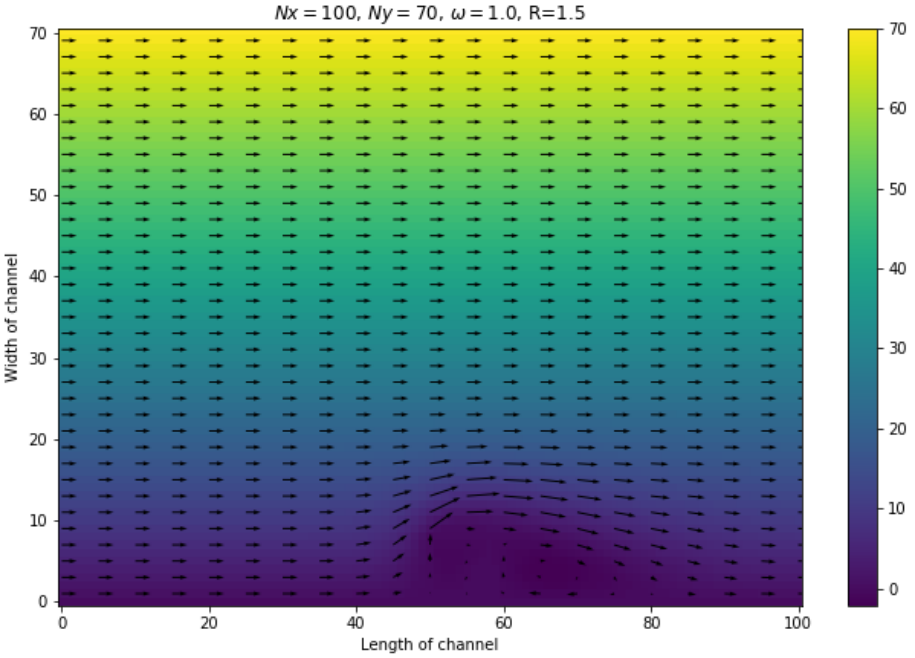

Conclusions

The pattern of flow of a fluid inside a channel with and without a blockage was investigated. With no blockage on the path, it is possible to obtain an analytic solution by imposing certain assumptions, such as no-slip boundary conditions. All assumptions are explained earlier in the report. The analytic approach results in a steady state solution with the form of the velocity along the channel being a parabola dependent on the height of the channel. The velocity is the greatest at the centre. Following this, numerical solutions were obtained using a finite difference method together with SOR. The solution develops gradually along the channel. By comparing the velocities at the outlet of the channel for the numerical and analytic case, the level of convergence is determined. The channel should be long enough for convergence to fully occur. The most efficient relaxation parameter was found to be $\omega = 1.2$.

When a beam is placed inside the channel, the effects of viscosity and of advection become important. This flow is assumed to be symmetric about the centreline of the beam, therefore only half of the plane is shown in all plots.

In fluid dynamics, the Reynolds number plays a huge part in determining the pattern of flow of a fluid. Reynolds number determines whether the advective term, $(\mathbf{v}\cdot\nabla)\mathbf{v}$ or the viscous term, $\nu\nabla^2\mathbf{v}$, of the Navier-Stokes Equation (quoted again below) predominates.

$$(\mathbf{v}\cdot\nabla)\mathbf{v} + \frac{\partial \mathbf{v}}{\partial t} = \mathbf{F} + \nu\nabla^2\mathbf{v} - \frac{1}{\rho}\nabla p$$

For low Reynolds number (for low fluid speed), the viscous term is more effective. Viscosity acts as a frictional force and smoothens the flow, therefore laminar flow is observed for the fluid. This result has been illustrated clearly in fig.(3.3) and fig.(3.4). In the latter, by extending the channel downstream of the beam, the laminar channel flow analogous to the flow in the first part of the investigation is retrieved further downstream of the beam.

The effect of increasing R on the flow has been investigated in an attempt to observe the flow when the advective term predominates. For $R = 1.5$, it is possible to see a clear vortex in the flow by inspecting the corresponding stream and contour plots in fig.(3.6).

In future investigations, the effects of increasing the inlet velocity could be investigated. Furthermore, a spherical beam could be used instead of a square beam. The beam could also not be placed symmetrically at the middle of the flow to investigate the differences in the pattern that would form.

Bibliography

[1] Batchelor, G. *An Introduction to Fluid Dynamics (Cambridge Mathematical Library)*. Cambridge: Cambridge University, pp.145-150, 2000.

[2] Majda, A. and Bertozzi, A. *Vorticity and incompressible flow*. New York: Cambridge University Press, pp.43-85, 2002.

[3] Landau R.H., Paez M.J. and Bordeianu C.C. *A Survey of Computational Physics*. Princeton University Press, pp.386-413,pp443-459.,2008.

[4] Weisstein, E. Successive Overrelaxation Method – from Wolfram MathWorld. [online] Mathworld.wolfram.com. Available at: http://mathworld.wolfram.com/SuccessiveOverrelaxationMethod.html [Accessed 19 Feb. 2019]